Reciprocal diagrams for membrane structures, an intuitive approach for membrane form-finding

Dongyuan Liu[*], Julian Lienhard[a]

[*]Tragwerksentwurf (TWE)

Universitätsplatz 9, 34127 Kassel, Germany
liu@uni-kassel.de

Abstract

In this paper, a connection between reciprocal diagrams and typical features in membrane structures is drawn. Although numerous form-finding techniques have been developed in the field of tensile membrane structures, the introduction of reciprocal diagrams allows for an intuitive understanding and can therefore facilitates the development in early design stages.

To begin with, we introduce relevant basic concepts, including planar reciprocal diagrams and force density method. The second part of the paper focuses on the construction of planar reciprocal diagrams for typical membrane features including membrane patches, ridge/valley cables (cables that go through a patch of membrane) and edge cables. The concept of anchoring force polygon is introduced. The third part of the paper discusses form-finding in 3D with force densities found in the planar reciprocal construction, followed by progressive steps of updating force densities based on current geometry. Several benchmark studies were undertaken. Comparisons to analytical solutions or finite-element results were done, showing good agreement.

Keywords: membrane structures, reciprocal diagrams, graphical methods, force density method, form finding, isotropic stress

1. Introduction

In the field of graphic statics, Maxwell's construction of 2D reciprocal diagrams (1) is a powerful tool for its clear presentation of form and force of an equilibrium system. The idea has been implemented in recent work in funicular vault structures (2), tensile membrane under vertical loading (3) and optimal trusses (4), among many others. This paper focuses on the reciprocal diagram construction of tensile membranes including typical features such as edge cables and ridge/valley cables, followed by the form finding process using the thereby informed force densities. The proposed method is fast and intuitive, rather straightforward to implement due to the use of 1D element only.

The current paper is organised as the following. First part of the paper reviews basic concepts of reciprocal diagrams (5), Frei Otto's edge cable technique (6) and the force density method developed by Schek (7). The second part extends Otto's technique to other features, namely ridge/valley cables and membrane patches. A complete construction of planar reciprocal diagram is therefore feasible. Here, Singer's extension of the classical force density method to membrane structures was inspirational (8). In the third and last part of the paper, lifting of the planar equilibrium was discussed, including a

progressive procedure of updating force densities. Several case studies are done and compared with analytical or finite-element results.

In the drawing of form and force diagrams, blue is used for compression and red for tension. Green denotes boundary conditions like anchoring forces or constraints. Black lines are used for constructional purposes, unless otherwise stated.

1.1. Reciprocal diagrams

The application of reciprocal figures in graphic statics is a powerful tool for its clear presentation of form and force in equilibrium. The 2D form and force diagrams share the same number of edges and can be constructed to any chosen angle regarding the corresponding pair of edges (5). Typically used are the parallel (Cremona convention) and orthogonal (Maxwell convention) constructions. This paper adopts the latter, as it remains the relative position of corresponding edges, enabling an intuitive reading of diagrams.
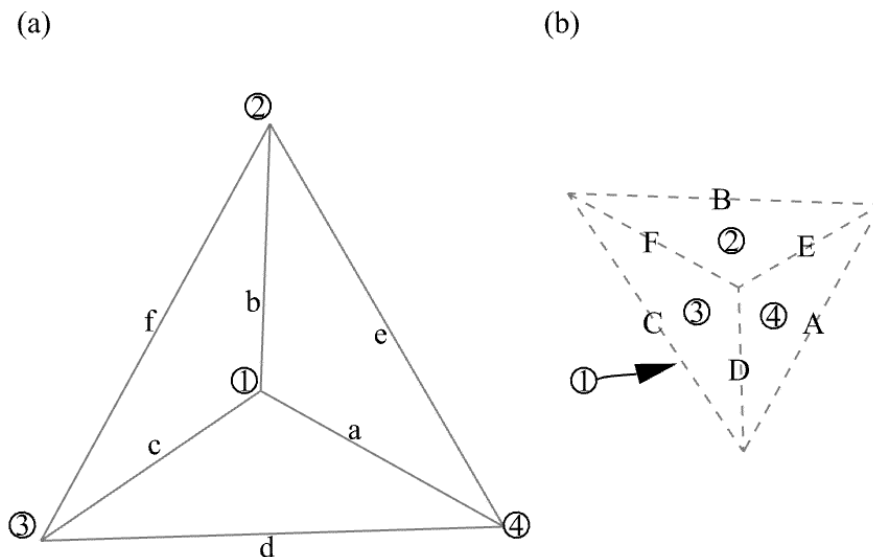

Figure 1. Reciprocal diagrams of an explanatory self-stressed truss following Maxwell convention. (a) Form diagram; (b) force diagram contain pairs of edges that are reciprocal to each other. The close polygons found in force diagram denote equilibrium in corresponding nodes in form diagram, e.g. triangle ② in (b) for node ② in (a).

1.2. Membrane edges of a planar isotropic stress field

Considering a planar membrane of isotropic stresses, namely same principal stresses without shear, the bending free edges, say materialised as edge cables, are of arc profiles. Such a planar stress field is also termed hydrostatic, like soup film (9). The analogy was widely used in Frei Otto's research of retractable membrane roofs (6), where the authors have drawn inspiration for the correlation to reciprocal diagrams, see section 2.1.

In the case of anisotropic stress with one dominating direction e.g., in warp pointing perpendicular to the span of an edge, the cable profile on the other hand follows a parabola profile. The difference of the two is diminishing as the sag to span ratio f/L (or rise) decreases. For a sensible rise around 10%, this can well be ignored. Mathematically, the Taylor series for the lengths of both arc and parabola profiles s_a and s_p tells no difference within the second order of sag f. In practise therefore, $L + \frac{8f^2}{3L}$ is often considered a good approximation for the cable length, Eq. (1) and (2). In this paper, we consider primarily form-finding for isotropic stress fields.

This preprint research paper was submitted on 27-Mar-2024 and has not been peer reviewed.

$$s_a = L + \frac{8f^2}{3L} - \frac{32f^4}{15L^3} + O(f^5)$$

(1)

$$s_p = L + \frac{8f^2}{3L} - \frac{32f^4}{5L^3} + O(f^5)$$
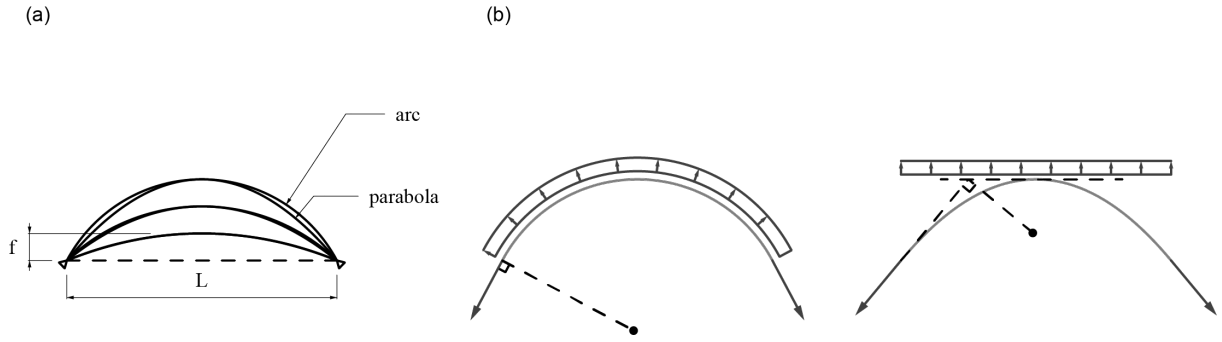
(2)

Figure 2. Edge representation of arc and parabola (a) geometries of different rises (sag to span ratio of 10%, 20% and 30%), (b) isotropic vs. directional membrane stress conditions. Black dot represents the centre and focal point respectively.

1.3. Force Density Method

Force density method (FDM) is a form-finding method developed initially for cable net structures such as the Olympic stadium roof in Munich (7). The form i.e., 3D coordinates of free nodes can be linearly solved with equilibrium condition only, given anchor point positions, external loads, and force densities in a net. In the absence of external loads, the linear equation of FDM reads:

$$C^T Q C_i x_i = -C^T Q C_f x_f$$

(3)

with $C = \begin{bmatrix} C_i & C_f \end{bmatrix}$ being the branch-node matrix of the network, Q the diagonal matrix of force densities, and $x^T = \begin{bmatrix} x_i^T & x_f^T \end{bmatrix}$ the coordinates, where subscript i designates free nodes and f for fixed nodes.

FDM has been extended for surface structures of isotropic stress field since late 20th , (8), (10) which had inspired the connection between a triangular membrane element and its reciprocal diagram in this paper. This is further discussed in section 2.3.

2. Planar reciprocal diagrams for membrane structures

Three types of building elements, namely edge cables, ridge/valley cables, and the membrane patches are considered. The reciprocal construction shown here demonstrates their form and force clearly which leads to an intuitive design procedure.

2.1. Edge cables and the anchoring force polygon

Considering a membrane corner anchoring two edge cables as the following Figure 3. As discussed, when the stress field is isotropic, the edges are of arc profiles. The well-known formular for

3

hydrostatic pressure $F = p \cdot r$, gives the constant cable force F as the product of pressure p and radius r. Assuming a membrane stress of unity, the edge cable forces $\overrightarrow{AD}$ and $\overrightarrow{AE}$ has the amplitude of its radius r_1 and r_2, pointing tangentially to their respective arc profiles. The anchoring force $\overrightarrow{AB}$ as the summation of these two cable forces, is in the direction of the *shared chord* $\overline{AC}$, and has the amplitude of $|O_1O_2|$. This can be proven by checking the congruence of $\triangle\, AO_1O_2$ and $\triangle$ DAB (11).

One shall notice, the form edge $\overline{AB}$ and the force edge $\overline{O_1O_2}$ constitute a reciprocal pair, sitting orthogonally to each other.
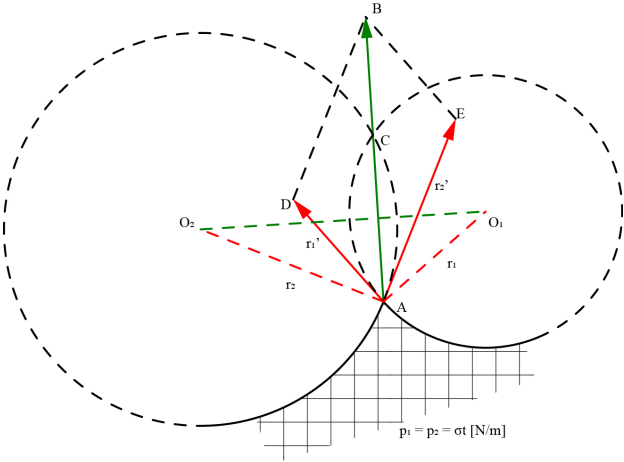
Figure 3. Graphical solution of anchoring force of two edge cables of arc profile at an anchor point A, with an isotropic stress field of unity.

With such, an anchoring force polygon (green dashed) can be constructed given a series of edge cables spanning an isotropic stress field of unity by simply connecting the centres consecutively. The amplitude and direction of planar anchoring forces at these anchor points are thereby determined graphically.
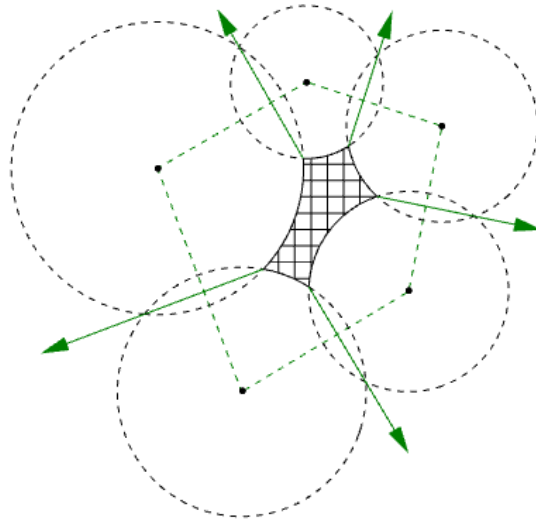
4

Figure 4. Anchoring force polygon (green dashed) of an isotropic stress field of unity in plane.

2.2. Ridge/valley cables

In addition to two edge cables at an anchor point as discussed in previous case, oftentimes a ridge/valley cable is present. That is, a cable spanning inside a membrane patch. Such cables can be used to adjust the membrane shape, deviating it from soup-film like geometries, which extends the design space of membrane structures.

The construction of reciprocal diagrams of ridge/valley cables can be done by "shifting" the diagrams apart. This correlates physically to the fact that the additional forces introduced by the ridge/valley cables need to be anchored, see the increase in amplitude of anchoring force edge (green dashed) between (a) and (b) in following Figure 5. The equilibrium is now denoted by the quadrilateral force polygon in Figure 5 (b), as opposed to the force triangle in Figure 5 (a). Note that the added ridge/valley cable does not have to be colinear with the existing anchoring cable, in other words it may alter the previous anchoring cable direction.
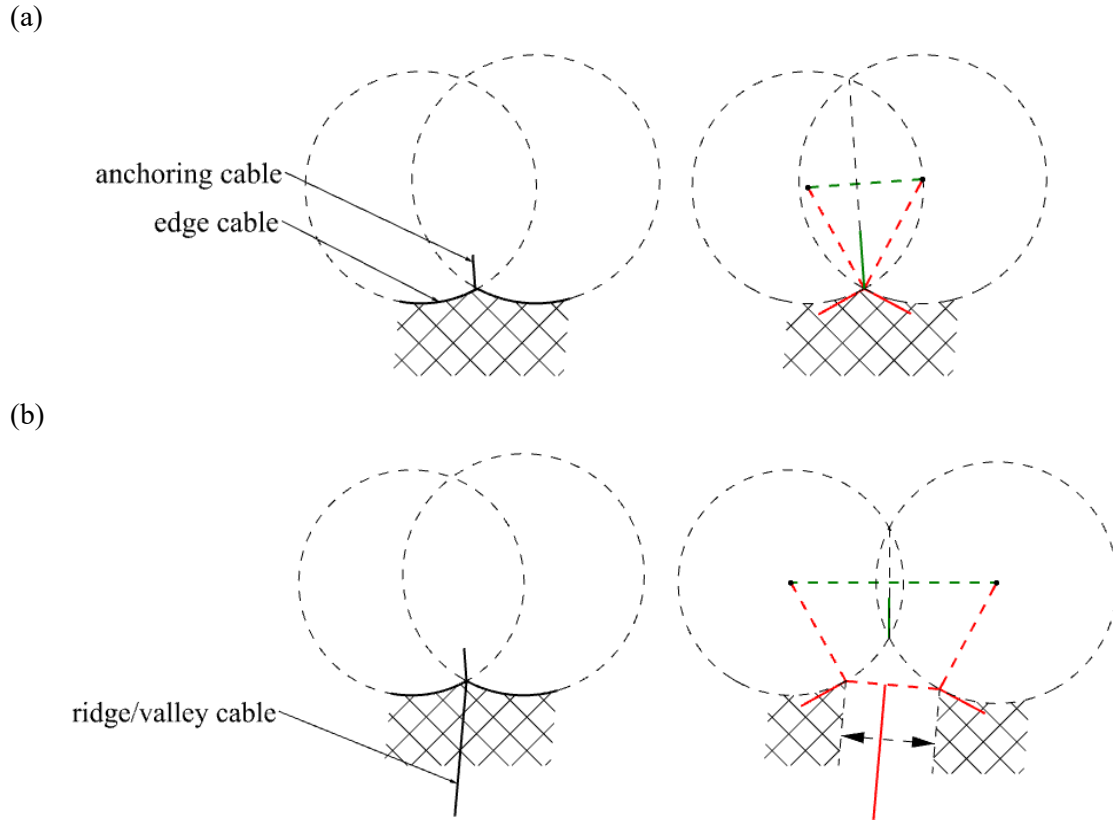
5

(a)

(b)

Figure 5. Reciprocal construction of ridge/valley cable in addition to two edge cables at one anchor point. equilibrium is now denoted by the quadrilateral force polygon in Figure 5 (b), as opposed to the force triangle in Figure 5 (a).

2.3. Membrane patches

After the discussion of typical cable elements in membrane structures, let's now turn to the membrane patch itself. A planar membrane patch subjected to isotropic stress of σ is discretised into a tri-mesh, a part of which shown as Figure 6 (a). Inspired by Singer's work on extended FDM for surface structures (8), the following reciprocal construction can be done. That is, the force introduced by a triangular face on one of its three vertices V_i, is perpendicular to the opposing edge E_i, and its amplitude equates $\frac{1}{2}\sigma l_i$, with l_i the length of E_i, i=1,2,3. Note that the tri-mesh is neither form nor force diagram. This enables the lumping of stresses to forces on the tri-mesh nodes, and therefore the use of 1D element only.

When the isotropic stress is unity i.e., $\sigma = 1$, the force diagram of this triangular face is simply its medial triangle as Figure 6 (c), and the corresponding form diagram is obtained by connecting the orthocentre of this face to its three vertices as Figure 6 (b).
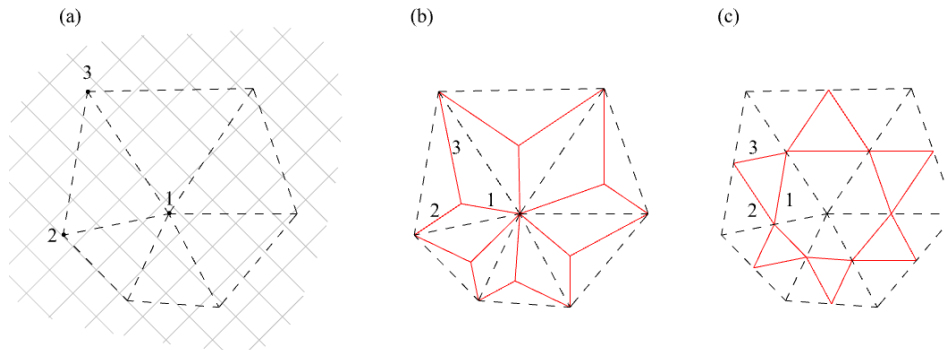
Figure 6. Reciprocal construction of tri-mesh under isotropic stress of unity: (a) tri-mesh, (b) form diagram, (c) force diagram. Note that the tri-mesh is neither form nor force diagram.

One shall notice the above construction gives three tension edges for an acute triangular face. In the case of an obtuse face, whereby the orthocentre sits outside, the constructed force edges are one compression edge and two tension edges. In the very special case of an orthogonal triangle, which practically would not be encountered in a regular discretization, only gives two meaningful tension edges. Numerically, the third edge of zero length and infinite force density, is one that starting from a node and ending at itself. Its corresponding row can be eliminated from the branch-node matrix. Physically, this zero-length edge has infinite geometric stiffness but no length to "exhibit" any forces.
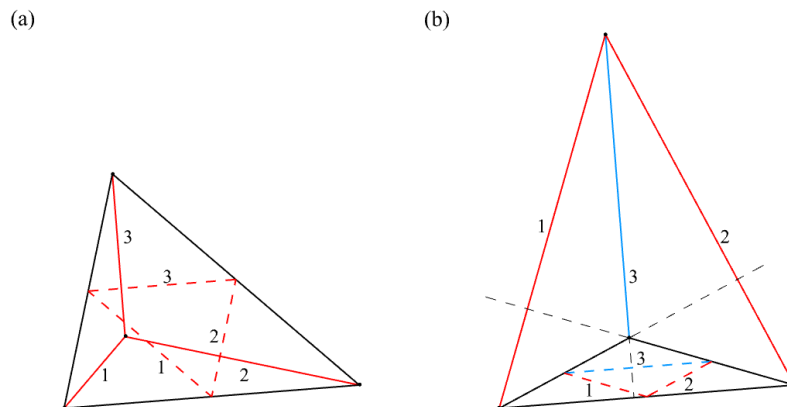

Figure 7. For an obtuse triangular face (b) whereby the orthocentre sites outside, the form edge through the obtuse vertex corresponds to a compression force.

2.4. Compatibility of features

Until now the construction for three components, namely edge cables, ridge/valley cables and membrane patches are described. Their form and force edges are compatible (in the sense that they do not overlap) given a triangular discretization which embeds the cable elements. The form edges of cable elements sit always on the tri-mesh edges, whilst the form edges for membrane patch sit always off the tri-mesh edges (with the exception in an orthogonal triangle as mentioned). This simplify the computational implementation of the method since no special topological manipulation is needed.

In terms of the force diagram, the compatibility (denoting equilibrium) is naturally given during the construction of close force polygons. For edge cables, their force edges share a "pole" i.e., the centre of their arc profiles. For patches, the median triangles denote the internal equilibrium of the tri-mesh faces. For ridge/valley cables, the choosing of prestressing forces are subjected to the designer, given the summation of these additional forces alone do not violate condition of equilibrium.

The introduction of ridge/valley cables causing a "shifting" effect in the force diagram, is in a similar fashion as adding creases in a funicular vault as described by Rippmann (12).
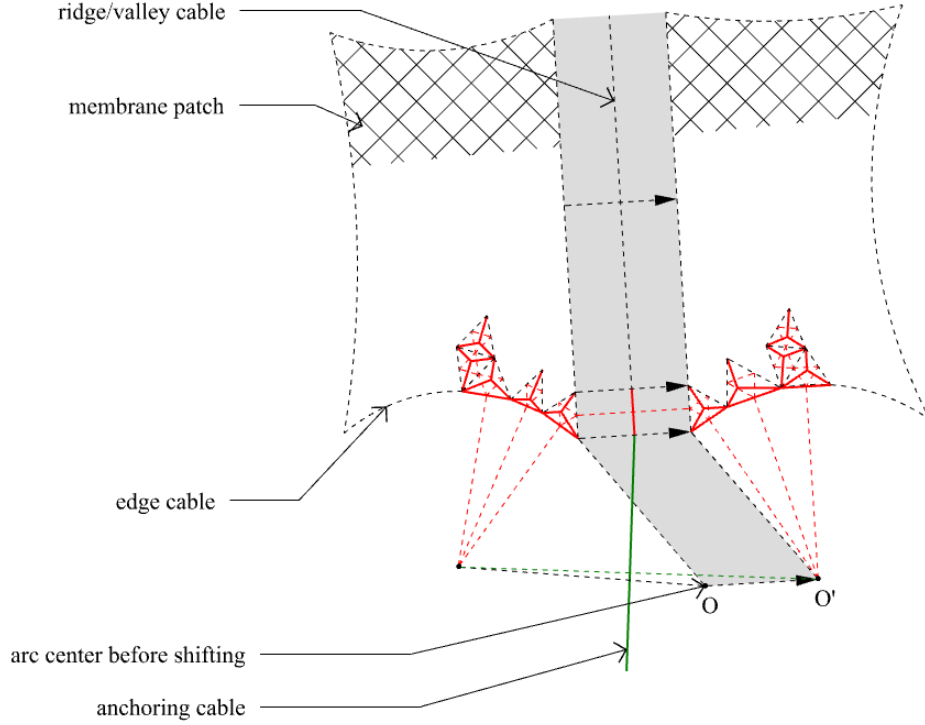
Figure 8. Compatibility of membrane features in the reciprocal diagram construction: coloured solid lines for form edges and coloured dashed lines for force edges. Introduction of ridge/valley cables "shift" the force diagram apart.

3. 3D form-finding and comparison of results

The planar equilibrium described by the constructed form and force diagrams presents a set of force densities for the given network. A linear FDM can therefore be used to lift the geometry into 3D when new anchor point heights are prescribed. A lift with only vertical displacement to approach a minimum surface is a practically meaningful approach, since the planar equilibrium is preserved when projected back, e.g. in cases where the force direction in plan is of primary importance. By lifting, the length of a form edge is increased by factor $1/cos(\theta_b)$, where θ_b is the angle between that bar b and the plane for reciprocal construction. The corresponding force has to increase by the same factor for the invariant force density. In more general cases where displacement is not restricted to vertical, this factor is also known as deformation gradient F.

In both cases, the lifted geometry does not correspond to an isotropic stress field anymore, see formulation by Bletzinger (13). The resulted non-isotropic stress field S, referring the deformed/actual geometry, is related to the imposed isotropic stress σ by F through $S = det F F^{-1} \cdot \sigma \cdot F^{-T}$. For 1D-elements (14), we have $F = l/L$, hence actual stress $S = \frac{L}{l}\sigma$, where l and L are the actual and reference bar lengths respectively. To summarize these relations within a tri-mesh face:

$$\frac{1}{2}\sigma = q_i = \frac{N_i}{L_i} = \frac{n_i}{l_i} = \frac{1}{2}\frac{l_i}{L_i}S_i, i = 1,2,3 \quad [N/m]$$
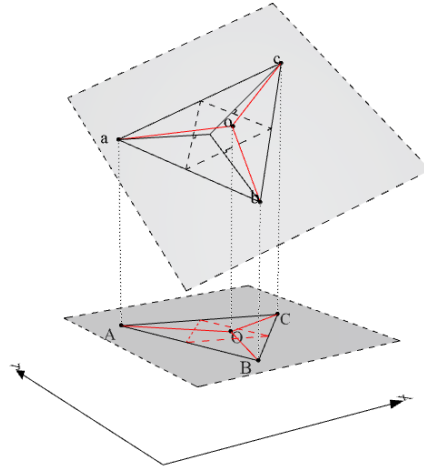
(4)

8

Figure 9. A visual hint: the lifted net (ao-bo-co) does not correspond to an isotropic stress field anymore (not perpendicular to median triangle of actual geometry △abc). Shown here is the case with vertical displacement only.

This can be resolved via a progressive procedure namely updating the force densities according to actual geometry. In other words, the planar equilibrium construction through reciprocals provides an intuitive entry point to find starting values for the following FDM steps, with many design intensions like the determination of anchoring forces, the introduction of ridge/valley cables already implemented.

This two-fold procedure is implemented in Python in Rhino3D®. For handling matrices, NumPy 1.24.2 (15) was used via "remote procedure call" mechanism provided by the COMPAS framework 1.17.5 (16).

3.1. Catenoid

Catenoid is a minimum surface of revolved catenary and can be analytically defined in cylindrical coordinates as the following. The code is tested with the geometry setup with two circular rings of 6 meters diameter, various distances apart. Solving constant c numerically with geometrical boundary conditions gives corresponding references.
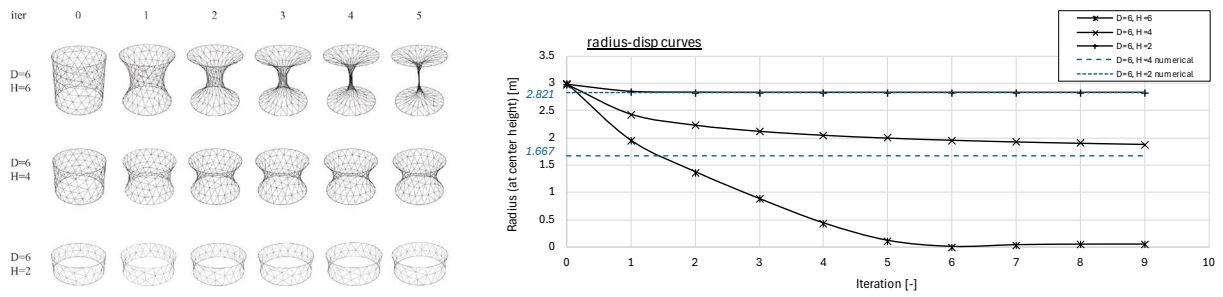
$$\rho = c \, cosh\frac{z}{c}$$

(5)

Figure 10. Geometries of step 1 to 5 of various catenoid setups and the radii plot over progressive steps of FDM (at centre height).
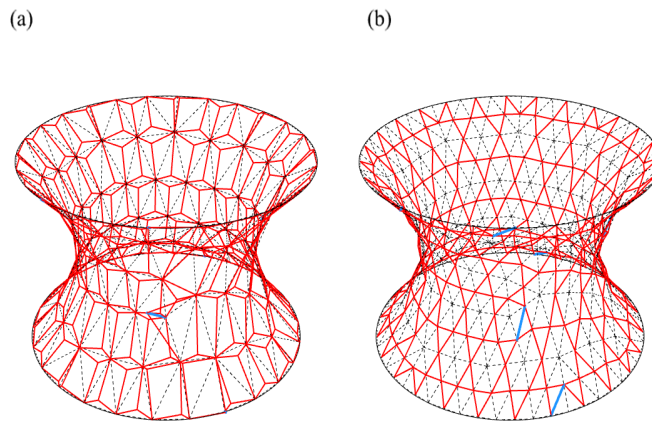

Figure 11. (a) Form diagram and (b) force diagram of catenoid D6H4, step 5.

It's well known that minimum surfaces cannot be found for all boundaries, e.g. when the rings are too far apart. In engineering practices, ridge/valley lines can be employed (17). Following case implements four ridge lines of 5 kN prestress, on the "D6H6" boundaries (ring diameter 6 meters and distance of 6 meters). Membrane prestress is an isotropic stress of 1 kN/m.
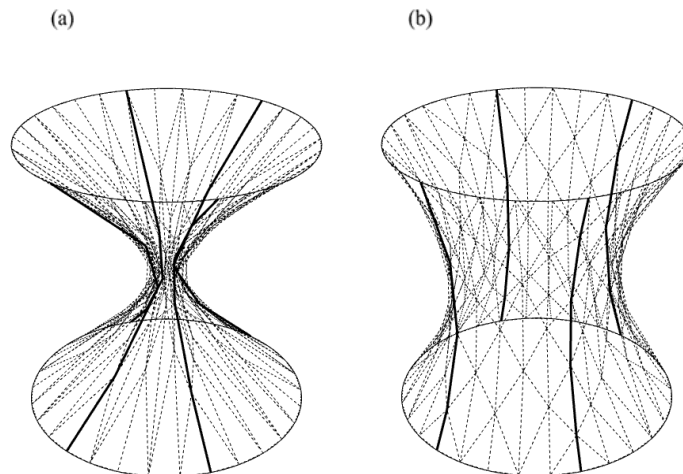

Figure 12. Testing results of ridge lines on otherwise collapsing "D6H6" catenoid. (a) no cable force assigned resulting in a collapsing minimum surface. (b) Assigning 5 kN of prestress in ridge cables.

3.2. A 4-point sail

The following example of a 4-point sail is aimed to further demonstrate the construction of planar reciprocal diagrams, with implementation of a ridge line, and the results are compared with program Kiwi!3D (18). The sail has a grid of about 9 meters span.

As mentioned, the form-finding starts from planar definition of features and reciprocal diagrams construction. We see here the difference of force diagram and the form found geometries after assigning of an 8 kN prestress in the ridge cable, which is also compared to the reference modelled in Kiwi!3D.
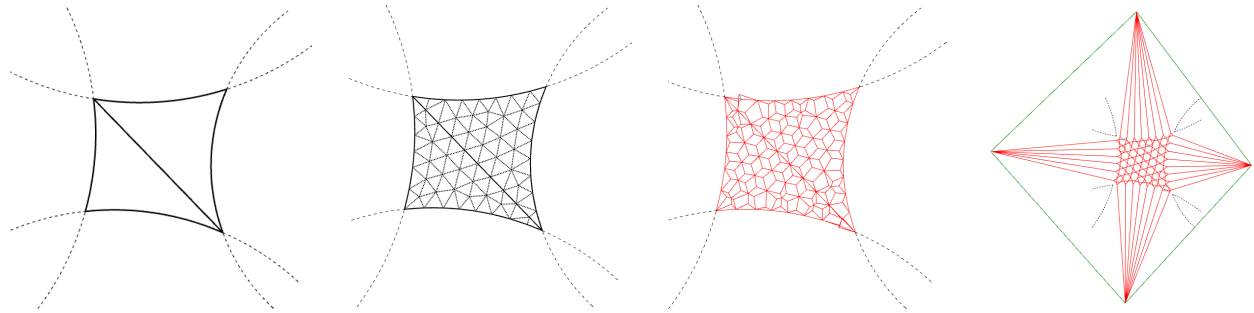

Figure 13. Planar reciprocal construction of tri-mesh under isotropic stress of unity: feature definition of edges cables (arcs) and ridge cables (lines), tri-mesh discretization, form diagram and force diagram, left to right. Note that at this stage a planar state of equilibrium is already found. All forces and geometries are known. Here no force is assigned to the ridge cable.
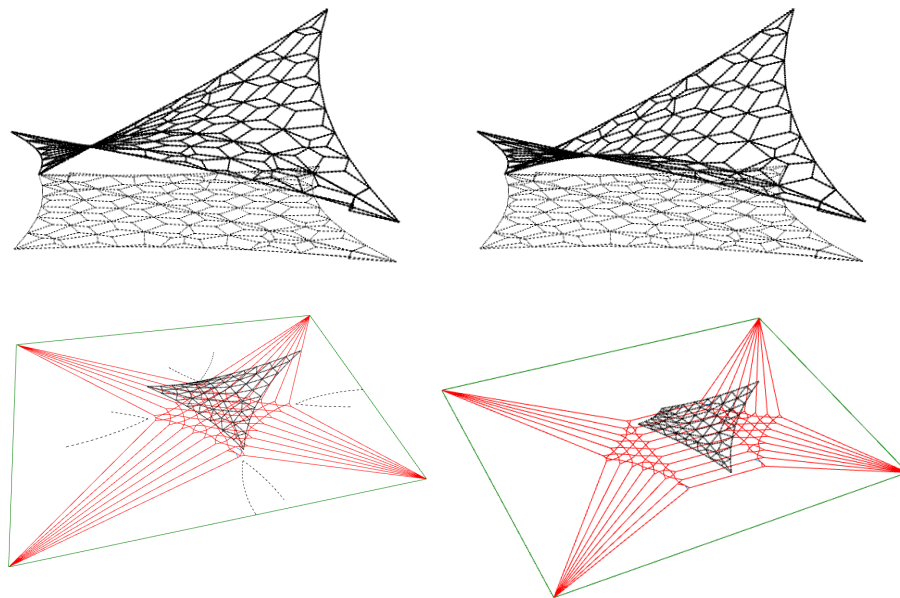

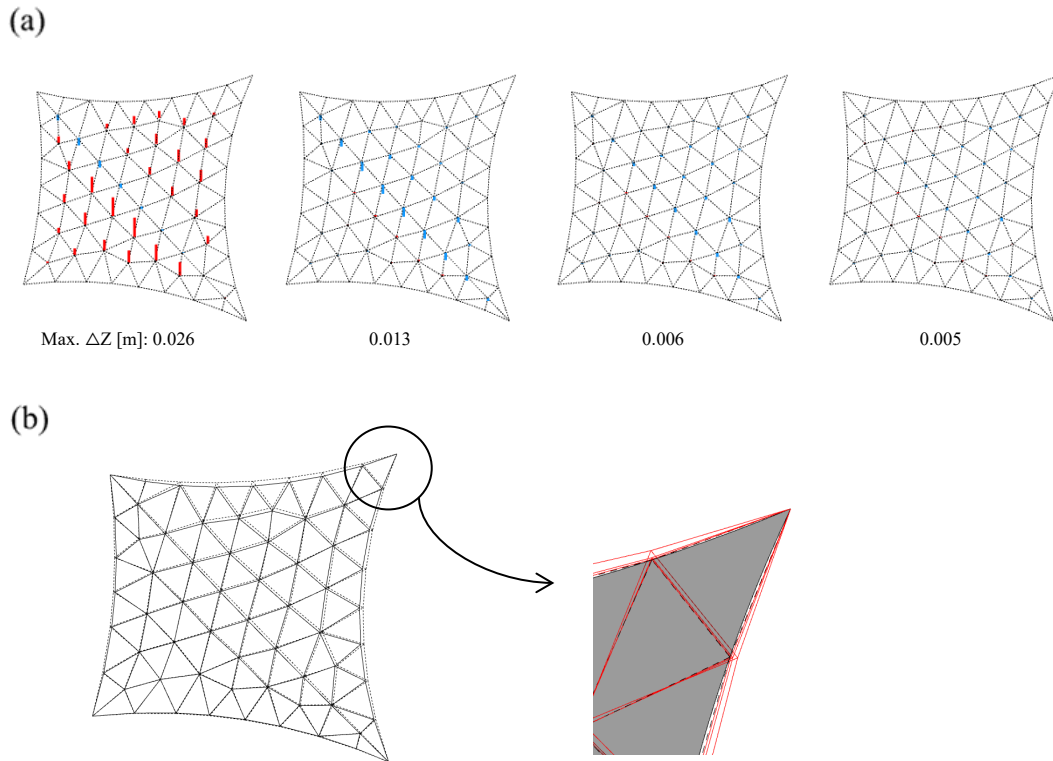Figure 14. Assigning an 8 kN prestress in ridge cable shifts the planar force diagram apart.

Figure 15. (a) Maximum height differences between Kiwi!3D (as reference) and FDM results, step 1 to 4. Red lines indicate reference is lower, blue being that reference is higher in vertical direction Z. (b) In plane (XY) difference: geometries of edge cables converge towards reference by Kiwi!3D (black surface in zoom-in diagram).

3.3. A twin-hypar

This example of a twin hypar is adopted from the "round-robin test" exercise 4 by Gosling and others (19) where several membrane structures were analyzed independently and compared, to "assess level of consistency and harmony in current practice" back in year 2013. In this example, the grid size is 6 by 6 meters, consisting of three high and three low points with 4 meters height difference. The membrane prestress is 5 KN/m in both warp and fill directions, and pretension of edges cables is 50 kN. A membrane prestress of non-unity makes no difference in the construction of reciprocals and therefore the finding of initial force densities, only that the forces assigned to those form edges of the membrane patches and edge cables are now simultaneously scaled.
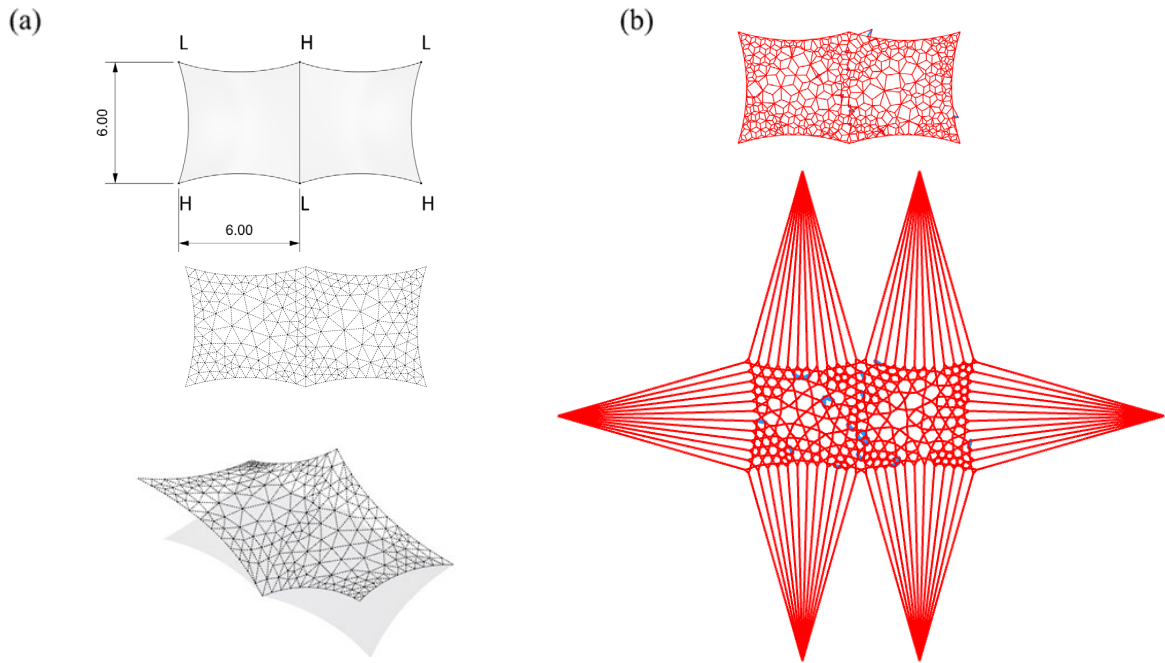
12

Figure 16. (a) Geometric layout of the twin hypar, initial tri-mesh, and form-finding result of iteration step 4 from top to bottom. (b) Initial planar form and force diagrams.

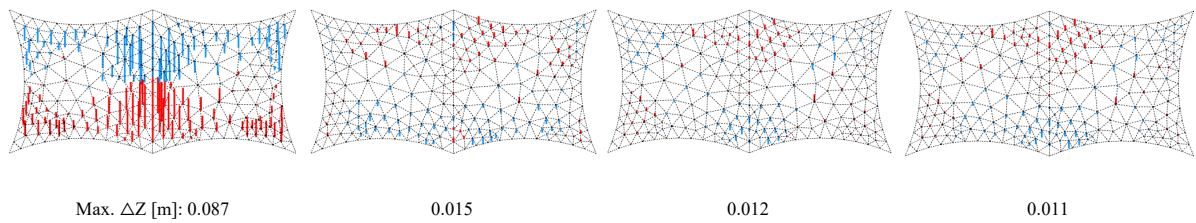| Max. $\triangle Z$ [m]: 0.087 | 0.015 | 0.012 | 0.011 |

Figure 17. Maximum height differences between Kiwi!3D reference geometry and FDM results, step 1 to 4. Red lines indicate reference is lower, blue being that reference is higher in vertical direction Z.

4. Conclusions

The current paper introduced a force density-based form-finding method for membrane of isotropic stress field, with edge and/or ridge cables. The main feature is the use of planar reciprocal diagrams as a starting point to find initial force densities, which enables a direct tuning of important design parameters like anchoring forces and ridge cables in the first design sketches. The equivalence of isotropic stress field to the lumped forces enabled the sole use of 1D elements. A progressive procedure, i.e. updating force densities based on current geometry after each linear solving step provided good agreement to references.

Declaration of conflicting interests

The authors declare that there is no conflict of interest.

13

Acknowledgements

References

1. Maxwell JC. I.—On Reciprocal Figures, Frames, and Diagrams of Forces. Earth and Environmental Science Transactions of The Royal Society of Edinburgh. 1870 ed;26(1):1–40.

2. Block P (Philippe CV. Thrust Network Analysis : exploring three-dimensional equilibrium [Internet] [Thesis]. Massachusetts Institute of Technology; 2009 [cited 2022 Dec 9]. Available from: https://dspace.mit.edu/handle/1721.1/49539

3. Van Mele T, Block P. A novel form finding method for fabric formwork for concrete shells. Journal of the International Association for Shell and Spatial Structures. 2011 Dec 1;52.

4. Baker W, Beghini L, Mazurek A, Carrion J, Beghini A. Maxwell's reciprocal diagrams and discrete Michell frames. Structural and Multidisciplinary Optimization. 2013 Aug 1;48.

5. Maxwell JC. XLV. On reciprocal figures and diagrams of forces. The London, Edinburgh, and Dublin Philosophical Magazine and Journal of Science. 1864 Apr 1;27(182):250–61.

6. Institut für leichte Flächentragwerke. IL5 Wandelbare Dächer Convertible Roofs. 1971.

7. Schek HJ. The force density method for form finding and computation of general networks. Computer Methods in Applied Mechanics and Engineering. 1974 Jan 1;3(1):115–34.

8. Singer P. Die Berechnung von Minimalflächen, Seifenblasen, Membrane und Pneus aus geodätischer Sicht [Diss.]. [Institut für Anwendungen der Geodäsie im Bauwesen]: Universität Stuttgart; 1995.

9. Wagner R. Basics in Tension Structures. International Journal of Space Structures. 2009 Dec;24(4):223–31.

10. Maurin B, Motro R. The surface stress density method as a form-finding tool for tensile membranes. Engineering Structures. 1998 Aug 1;20(8):712–9.

11. Liu D, Grünkorn G, Lienhard J, Chokhachian A, Auer T. Retractable membrane roofs as urban shading device. In: Proceedings of the TensiNet Symposium 2023 TENSINANTES2023. Nantes, France; 2023. p. 114–26.

12. Rippmann M. Funicular Shell Design: Geometric approaches to form finding and fabrication of discrete funicular structures [Internet]. ETH Zurich; 2016 [cited 2023 Apr 12]. p. 374 p. Available from: http://hdl.handle.net/20.500.11850/116926

13. Bletzinger KU, Ramm E. A General Finite Element Approach to the form Finding of Tensile Structures by the Updated Reference Strategy. International Journal of Space Structures. 1999 Jun 1;14(2):131–45.

14. Wüchner R, Bletzinger KU. Stress-adapted numerical form finding of pre-stressed surfaces by the updated reference strategy. International Journal for Numerical Methods in Engineering. 2005;64(2):143–66.

15. Harris CR, Millman KJ, van der Walt SJ, Gommers R, Virtanen P, Cournapeau D, et al. Array programming with NumPy. Nature. 2020 Sep;585(7825):357–62.

15

16. Mele TV, others many. COMPAS: A framework for computational research in architecture and structures. [Internet]. 2017. Available from: https://doi.org/10.5281/zenodo.2594510

17. Knippers J, Cremers J, Gabler M, Lienhard J, Cremers J, Institut für Internationale Architektur-Dokumentation, editors. Atlas Kunststoffe + Membranen: Werkstoffe und Halbzeuge, Formfindung und Konstruktion. 1. Aufl. München: Inst. f. Internat. Architektur-Dokumentation; 2010. 296 p. (Edition Detail).

18. Längst P, Bauer A, Michalski A, Lienhard J. The Potentials of Isogeometric Analysis Methods in Integrated Design Processes. In 2017.

19. Gosling PD, Bridgens BN, Albrecht A, Alpermann H, Angeleri A, Barnes M, et al. Analysis and design of membrane structures: Results of a round robin exercise. Engineering Structures. 2013 Mar;48:313–28.

20. Pauletti RMO, Fernandes FL. An outline of the natural force density method and its extension to quadrilateral elements. International Journal of Solids and Structures. 2020 Mar 1;185–186:423–38.